Available online at www.sciencedirect.com
SCIENCE DIRECT®
Journal of Colloid and Interface Science 272 (2004) 1–9
JOURNAL OF Colloid and Interface Science
www.elsevier.com/locate/jcis

# Stress development during drying of calcium carbonate suspensions containing carboxymethylcellulose and latex particles

Pär Wedin,[a,*] Carlos J. Martinez,[b] Jennifer A. Lewis,[b] John Daicic,[a] and Lennart Bergström [a]

[a] *YKI, Institute for Surface Chemistry, P.O. Box 5607, SE-11486 Stockholm, Sweden*
[b] *Department of Materials Science and Engineering, University of Illinois, Urbana, IL 61801, USA*

Received 17 April 2003; accepted 12 December 2003

**Abstract**

Stress development during drying of coatings produced from aqueous dispersions of calcium carbonate particles in the presence and absence of organic binders was studied using a controlled-environment stress apparatus that simultaneously monitored drying stress, weight loss, and relative humidity. Specifically, the influence of two organic binders on drying stress evolution was investigated: (1) carboxymethylcellulose, a water-soluble viscosifying aid, and (2) a styrene–butadiene latex emulsion of varying glass transition temperature. The stress histories exhibited three distinct regions. First, a period of stress rise was observed, which reflected the capillary tension exerted by the liquid on the particle network. Second, a maximum stress was observed. Third, it was followed by a period of either stress decay or rise depending on the organic species present. Significant differences in stress histories were observed between coatings containing soluble and nonsoluble binders. Maximum drying stresses ($\sigma_{max}$) of 0.2–0.5 MPa were observed for coatings produced from pure calcium carbonate or calcium carbonate–latex suspensions, whereas coatings with carboxymethylcellulose exhibited substantially higher $\sigma_{max}$ values of 1–2 MPa. Upon drying, these coatings were quite hygroscopic, such that cyclic variations in relative humidity induced large cyclic changes in residual stress.


*Keywords:* Calcium carbonate; PCC; CMC; Carboxy methylcellulose; Latex; Drying; Paper coating; Stress evolution

## 1. Introduction

Colloidal suspensions containing soluble and nonsoluble organic binders are used in numerous technological applications including paper coatings [1,2], paints [3,4], inks, and as precursors to a wide variety of ceramic materials [5,6]. Paper coatings, for example, are complex formulations that typically contain pigment particles, latex binders, and soluble viscosifying additives (such as cellulose binders) in an aqueous suspension. Paper coatings add value to the final product by enhancing print properties, opacity, brightness, or gloss. Liquid removal, or drying, is a critical step in the coating process. The coating structure evolves during drying, as the capillary tension in the liquid phase exerts a compressive force on the particle network driving its consolidation. Stress develops during drying due to the constrained volume shrinkage associated with loss of liquid from the coated layer, which can promote defect formation such as cracks, warping, mottling, or phase segregation.

In related work, Chiu et al. [7,8] and Guo and Lewis [9] have studied drying of coatings produced from aqueous colloidal suspensions of varying stability. They carried out in situ drying stress measurements on coatings derived from stable and flocculated dispersions without organic binders and correlated the measured stress to that induced by capillary tension in the liquid phase. Such coatings exhibited a period of stress rise, followed by a maximum stress, and a subsequent decline to a stress-free state. Chiu and Cima [8] showed that the maximum stress coincided with the point where consolidation of the particle network ceased, i.e., where the liquid–vapor interface first began to recede into the coating. They identified several processing parameters that influenced the drying stress evolution and cracking behavior of such films. Of these, particle size, liquid surface tension, and dispersion stability had the most pronounced influence on drying behavior.

More recently, Lewis and co-workers [6,10] have studied the effects of organic binder additions on the drying behav-

* Corresponding author.
*E-mail address:* par.wedin@surfchem.kth.se (P. Wedin).

0021-9797/$ – see front matter 
doi:10.1016/j.jcis.2003.12.030

ior of coatings produced from both aqueous and nonaqueous colloidal suspensions. Specifically, two systems were investigated, one based on nonaqueous tape-casting formulations that contained poly(vinylbutyral), a soluble organic binder [6], and the other based on aqueous binary mixtures composed of rigid silica microspheres and deformable acrylic latices [10]. They observed significant differences in the drying stress histories of tape-cast layers in the presence and absence of soluble organic binders, which were mirrored by the stress histories of the corresponding pure binder coatings. For example, they found that substantial stresses continued to build in these coatings long after the liquid–vapor interface receded into their interiors. Their observations served to highlight the important role that soluble organic species play in stress development. In contrast, coatings produced from binary mixtures of rigid colloidal particles and deformable latices exhibited features characteristic of pure particulate coatings during the initial rise to their maximum stress. However, their subsequent stress relaxation was governed primarily by the organic phase, i.e., the latex glass transition temperature and the ratio of rigid to deformable particles. In such binary systems, films formed near the critical pigment concentrations exhibited the highest drying stresses.

The presence of organic binders clearly has a strong influence on the drying stress evolution of advanced coatings. However, little is known regarding the combined effects of having soluble and nonsoluble organic binders present in a given coating formulation, such as those utilized in paper manufacture. Although Petersen et al. [4] recently studied the drying stress evolution of coatings that contained pigment, acrylic latex, and a soluble binder, they neglected to account for possible contributions stemming from the soluble constituent.

Here, we aim to investigate the drying stress evolution of a model paper-coating system composed of calcium carbonate pigment particles, styrene–butadiene latex binders of varying glass transition temperature, and a soluble viscosifying additive composed of carboxymethylcellulose. In such systems, the pigment/binder volume ratio exceeds the critical pigment concentration, so that the dried coating will contain internal porosity. We show that the coating composition strongly affects the drying stress evolution, maximum stress, and residual stress. We found that coatings containing carboxymethylcellulose exhibited substantially higher maximum drying stress ($\sigma_{\max}$) values of 1–2 MPa, compared to the 0.2–0.5 MPa observed for coatings produced from pure calcium carbonate or calcium carbonate–latex suspensions. Further, the hygroscopic nature of the carboxymethylcellulose was seen to strongly affect the drying stress evolution, so that cyclic variations in relative humidity induced large cyclic changes in residual stress. We believe that our observations have important implications for the design and drying strategy of granular films such as paper coatings.

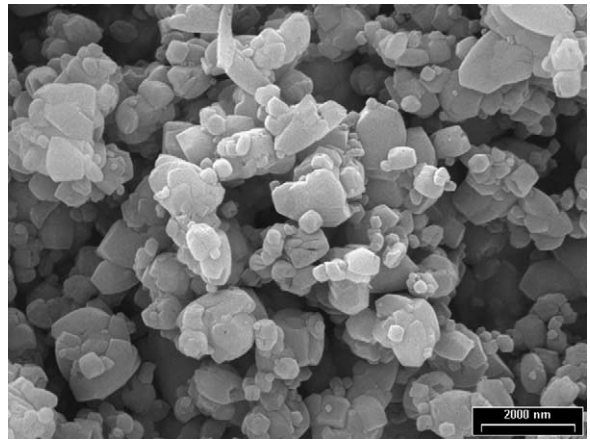


Fig. 1. SEM micrograph of the calcium carbonate powder.

## 2. Materials and methods

### 2.1. Materials system

The model system investigated in this study is an aqueous suspension containing three components: (1) precipitated calcium carbonate ($CaCO_3$) powder (Albagloss L PCC, Specialty Minerals, USA) stabilized with a sodium polyacrylate dispersant (NaPA, Dispex N40, Ciba Specialty Chemicals), (2) styrene–butadiene latices (DL 980 and XZ 943262, Dow Sverige AB, Sweden), and (3) carboxymethylcellulose (CMC, Finn-Fix 10, Metsä Specialty Chemicals Oy, Finland). The $CaCO_3$ powder, which served as the pigment phase, consists of irregularly shaped particles, as shown in Fig. 1. The mean particle size is 2.2 μm with 90% of the particles finer than 3.8 μm, as determined by light scattering (Mastersizer 2000, Malvern Instruments), and their specific surface area is $\sim$4.0 $m^2/g$, as determined by nitrogen gas adsorption (Model ASAP 2400, Micrometrics). Two styrene–butadiene latices, denoted as L- and H-latex for particles with glass transition temperatures ($T_g$) of $-7$ and 28 °C, respectively, served as the nonsoluble binder phase. Both L- and H-latices have a narrow particle size distribution with a mean diameter of 0.14 μm. Carboxymethylcellulose, with a weight-average molecular weight of 60,000 g/mol, served as the soluble viscosifying aid (or thickener).

### 2.2. Suspension preparation

Calcium carbonate suspensions (at two different initial volume fractions, $\phi_{\text{initial}} = 0.21$ or $\phi_{\text{initial}} = 0.44$) were prepared by adding the appropriate amount of deionized water and dispersant to the powder, while mechanically stirring for 15 min at 500 rpm. If binder additions were made to the suspension, it was stirred for an additional 15 min at 1000 rpm per addition. Upon completion of the initial mixing process, the solution pH was adjusted to 8.5 and each suspension was stirred for another 60 min at 1000 rpm. Finally, each suspension was ultrasonicated for 10 min in an ultrasonic bath. Following this procedure, each suspension was magnetically

Table 1
Summary of the different dispersion formulations

| Sample No. | $\phi$ | $CaCO_3$ (wt%) | NaPA (wt%) | CMC (wt%) | Latex (wt%) |
|---|---|---|---|---|---|
| 01 | 0.21 | 41.8 | 0.13 | 0 | 0 |
| 02 | 0.44 | 67.9 | 0.20 | 0 | 0 |
| 03 | 0.21 | 41.6 | 0.12 | 0.42 | 0 |
| 04 | 0.44 | 67.4 | 0.20 | 0.67 | 0 |
| 05 | 0.21 | 35.0 | 0.10 | 0.35 | 3.5 (L-latex) |
| 06 | 0.44 | 58.7 | 0.18 | 0.59 | 5.9 (L-latex) |
| 07 | 0.21 | 35.0 | 0.10 | 0.35 | 3.5 (H-latex) |
| 08 | 0.44 | 58.7 | 0.18 | 0.59 | 5.9 (H-latex) |
| 09 | 0.21 | 35.1 | 0.11 | 0 | 3.5 (L-latex) |
| 10 | 0.44 | 59.0 | 0.18 | 0 | 5.9 (L-latex) |
| 11 | 0.21 | 35.1 | 0.11 | 0 | 3.5 (H-latex) |
| 12 | 0.44 | 59.0 | 0.18 | 0 | 5.9 (H-latex) |

Note that the volume fraction $\phi$ for samples 07–12 is the total $\phi$ for calcium carbonate and latex combined.

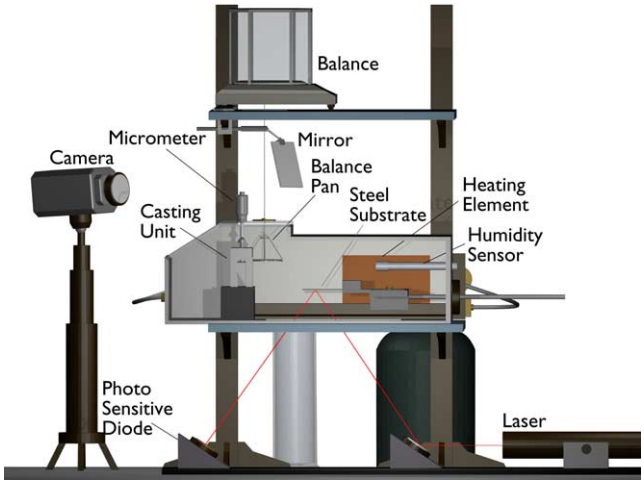


Fig. 2. Schematic illustration of the drying stress measurement apparatus.

stirred prior to coating formation. A detailed summary of all the coating formulations is provided in Table 1. The volumetric pigment/latex binder ratio for formulations 7–12 is 3.8, which is above the critical pigment volume fraction for this system.

### 2.3. Drying stress measurements

The stress histories of the coatings were measured in situ during drying using the cantilever deflection technique illustrated in Fig. 2. This device has an environmental chamber that allows both humidity (15–70% RH ± 1%) and temperature (22–35 ± 1 °C) control. Additional specifications are provided elsewhere [11,12]. This technique relates the end deflection of a clamped stainless steel substrate to the stress developed in an attached coating as it dries. The end deflection was measured using an optical ensemble consisting of a 1-mW helium laser (Uniphase, Model 1103), a position-sensitive photodiode (UDT Sensors, No. DL-10), an array of mirrors, and a data acquisition computer. Clean, polished substrates were mounted onto a movable sample holder fixed at one end. A calibration curve for each substrate was obtained by deflecting the free end of the substrate a known distance using a micrometer. Using a propagation of error analysis, the measurement error for this apparatus in term of stress units was estimated to be ∼0.010 MPa. Upon calibration, the steel substrate was positioned beneath a small doctor blade and the suspension was deposited onto the substrate with a syringe. This assembly was then moved beneath the doctor blade at a constant speed of 1 cm/s to create a coating of the desired initial thickness (240–520 μm, unless otherwise specified). A final film thickness of ∼100 μm was obtained for each coating. All coatings were dried at 30% relative humidity and a temperature of 25 °C. The biaxial, in-plane $(x - y)$ stress, $\sigma$, averaged across the coating thickness is related to the substrate deflection by [13]

$$\sigma = \frac{dEt_s^3}{3t_c l^2(t_s + t_c)(1-\nu)} + \frac{dE_c(t_s + t_c)}{l^2(1-\nu_c)}, \tag{1}$$

where $d$, $E$, $E_c$, $t_s$, $t_c$, $l$, $\nu$, and $\nu_c$ are the end deflection, elastic modulus of the substrate, elastic modulus of the coating, substrate thickness, film height, substrate length, Poisson ratio of the substrate, and Poisson ratio of the coating, respectively.

If the modulus of the coating is much smaller than the substrate modulus (as is the case for most particulate films on rigid substrates) this second term can be neglected without introducing significant error (∼1% or less) [13]. Therefore, only the first term in Eq. (1) was used for our stress data analysis. The stainless steel substrates used had a thickness of 254–400 μm and clamped dimensions of 50.8 × 6.35 mm with the following properties: $E = 190 \pm 20$ GPa, $l = 50.8$ mm, and $\nu = 0.36$.

There are several important considerations in applying the above equation to estimate internal stress development in latex-based films. First, the recorded stress histories must be corrected to account for the contribution of weight loss associated with water evaporation to the measured deflection. Because the film height changes during the measurement, the instantaneous film height early in the experiment is greater than the final height. The reported stress histories have been calculated using a final film thickness that represents an average value obtained by taking micrometer

measurements across the entire sample. Use of this average value yields a reasonable estimate of the maximum and residual stress for a given film. In our experiments, the final film thickness exceeded ∼1/3 of the substrate thickness. Payne [12] has shown that under these conditions the position of the neutral axis (plane in a bending plate where the strain is zero) within the coated substrate is shifted away from the location of $(t_s + t_c)/2$ assumed in Eq. (1) leading to a slight overestimate of the measured stress. Finally, stress distributions throughout the coating thickness that arise due to microstructural differences cannot be measured by this technique. For example, local variations in the deformation rate across such films would impact their instantaneous modulus. However, this property is not included in the first term of Eq. (1). In related work, Smay and Lewis [14] have shown that there is little compositional variation (in the $z$-axis direction) in latex-based composite films, indicating the absence of microstructural differences in later stages of the film formation process. However, in light of the above considerations, the reported data should be viewed in a qualitative manner, serving only as a guideline for establishing general trends between the films studied here.

Weight loss measurements were simultaneously carried out on duplicate samples in the cantilever stress chamber during the drying stress measurements. The weight loss data were acquired by suspending the coated substrate from a bottom-loading balance (Metler Toledo, Model AG204).

## 3. Results and discussion

### 3.1. $CaCO_3$ suspensions

The stress profiles and corresponding weight loss behavior during drying of pure calcium carbonate coatings are shown in Fig. 3. The stress evolution for the calcium carbonate coatings is representative of that observed for particulate films with little or no additive [8,9]. The stress increased rapidly to a maximum value, followed by a rapid stress relaxation to a nearly stress-free state. Changing the initial volume fraction of particles, $\phi_{\text{initial}}$, from 0.21 to 0.44 resulted in an increase of the maximum stress from 0.23 to 0.44 MPa.

At the onset of the drying process, the film is covered with liquid and the evaporation rate is constant. Initially, the particle network consolidates at the same rate as the pore liquid evaporates, resulting in negligible stress buildup. At some point the particle network will cease to consolidate, forcing the liquid to recede into the pores. Capillary pressure quickly builds up and creates a compressive stress in the film [15]. The maximum stress was reached when ∼66% and ∼31% of the initial water was removed from the films of low and high initial solids volume fraction, respectively. As evaporation proceeds, the liquid–vapor interface migrates into the granular film and the stress relaxes. We find that the evaporation rate was constant until more than 90% of the initial water

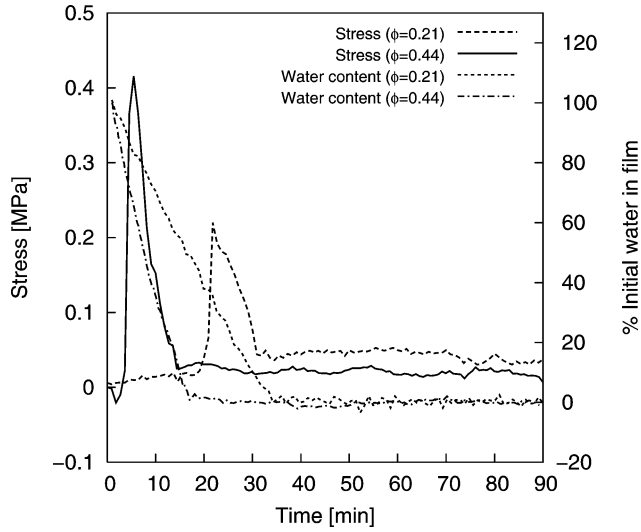


Fig. 3. The drying stress and water content as functions of the drying time for pure calcium carbonate films.

was removed from the films. Hence, the constant rate period, CRP, persisted beyond the stress peak, which suggests that it is external boundary conditions that determine the rate of evaporation, e.g., the diffusion of water vapor from the surface of the film to the surrounding media [15,16].

For particulate films it is possible to calculate the capillary pressure in the film using the Young–Laplace equation [17],

$$P_{\text{cap}} = \frac{2\gamma}{r_p}, \tag{2}$$

where $P_{\text{cap}}$, $\gamma$, and $r_p$ are the capillary pressure, the surface tension, and the pore radius, respectively. Since the tortuous capillary pores within the particle network have little in common with cylindrical tubes, an equivalent pore radius can be estimated by using the hydraulic radius, $r_h$, described by [18]

$$r_h = \frac{2(1-\phi)}{\phi\rho_s S}, \tag{3}$$

where $\phi$, $\rho_s$, and $S$ are the particle volume fraction, the density of the solid phase, and the specific surface area of the particles, respectively.

We find that the coating with higher initial solids loading consolidates to a higher volume fraction upon drying, with smaller pores as a consequence. The stress reaches a maximum value at solids volume fractions of $\phi \approx 0.41$ and $\phi \approx 0.47$ for the low and high $\phi_{\text{initial}}$ suspensions, respectively. By using a surface area estimated from the volume-average particle size ($D = 2.16$ µm), the capillary pressure is estimated to $P_{\text{cap}}$ ($\phi = 0.41$) $= 0.28$ MPa and $P_{\text{cap}}$ ($\phi = 0.47$) $= 0.36$ MPa, which is in fairly good agreement with the experimental data. Calculating the equivalent pore radius from the surface area measured by nitrogen gas adsorption gives unreasonably high capillary pressure. The polydispersity of the calcium carbonate powder means that the small particles contribute greatly to the specific surface area.

The $CaCO_3$ films did not relax to a completely stress-free state when drying was complete. In a previous study on silica suspensions, Guo et al. also found that the film displayed a residual stress and attributed this to the reprecipitation of dissolved salt in the pore liquid, forming salt bridges between particles. Calcite is partly soluble in water, 0.014 g/l at 25 °C [19], and the residual stress displayed for both of the calcium carbonate samples may be related to a similar reprecipitation of dissolved calcium carbonate at the particle contact points.

### *3.2. Addition of latex binder*

Figs. 4 and 5 displays the drying stress evolution for binary coatings containing $CaCO_3$ and latex binder. We find that addition of rigid latex particles (Fig. 4) results in a very sharp stress peak and virtually no residual stress. The maximum stress occurred when 96% and 94% of the water content was removed from the films of low and high initial solids volume fraction, respectively. It should be noted that the film thickness for the calcium carbonate system containing rigid latex particles at a low initial solids loading had to be reduced to avoid cracking, which means that it dried more quickly and reached the critical point sooner.

The drying stress curves for pure $CaCO_3$ coatings (Fig. 3) and binary coatings containing rigid latex particles (Fig. 4) are similar in shape. Addition of H-latex results in a slight increase in the maximum stress for the suspension at a high initial volume fraction. This suggests that addition of small, rigid latices results in only a slight increase in the capillary-induced stress, which probably is related to a smaller pore size. The rapid stress relaxation is typical of a dispersion of rigid particles [8,9]; the latex particles, having a $T_g$ above the experimental temperature, are simply too rigid to experience deformation during the film formation process.

The drying stress evolution for binary coatings containing the deformable latex particles is completely different (Fig. 5). The granular films containing deformable latices at a low initial solids loading exhibit a period of rise in tensile stress up to a maximum value of ∼0.22 MPa. The stress relaxes somewhat as evaporation proceeds beyond the first stress peak, but is then followed by a second stress rise period. The stress maximum is reached when ∼94% of the initial water content has been removed. Little stress relaxation is observed beyond this point; the final stress at 90 min is nearly equivalent to the maximum stress value.

The volume fraction at the first stress peak is $\phi \approx 0.37$ for the sample with low initial solids loading, compared to $\phi \approx 0.41$ for the corresponding calcium carbonate film, suggesting that the stress peak is induced by the capillary pressure in the pores at the end of the consolidation process. The point of maximum stress occurs at $\phi \approx 0.82$, an unlikely high solids loading for a saturated dispersion. It is more reasonable that the air starts to penetrate into the pores of the calcium carbonate particle network after the first stress peak, and the stress declines initially as a result. Due to the great difference in particle size between the latex and the calcium carbonate, the latex particles could still be fairly mobile in the remaining liquid. The second stress maximum and the associated stress plateau is probably related to the compression and coalescence of the soft latex particles [20,21].

Martinez and Lewis [10] studied the stress evolution of binary silica–latex films at different silica–latex ratios. They reported a smooth transition of the drying stress profile from a sharp peak with no residual stress for the pure silica system to a slow increase in the stress to a plateau of residual stress for the latex system. They saw no evidence of a two-step process. However, in their work, the silica and latex particles were of comparable size, thereby reducing the possibility of having latex coalescence some time after the stress peak induced by the capillary pressure in the particle network.

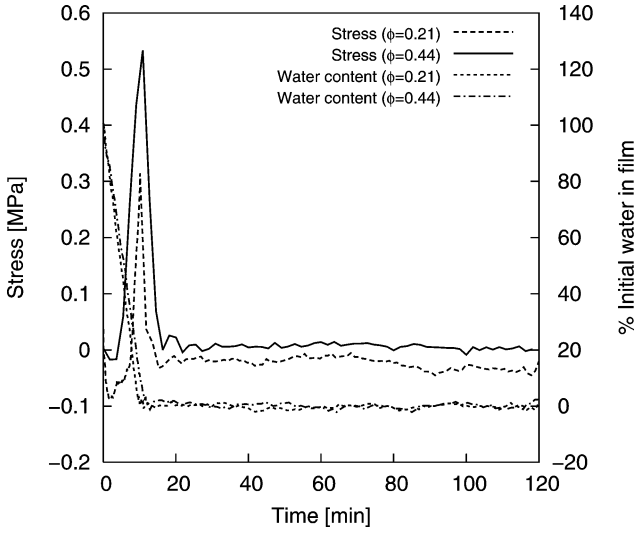


Fig. 4. The drying stress and water content as functions of the drying time for the binary films containing calcium carbonate and rigid latex particles.

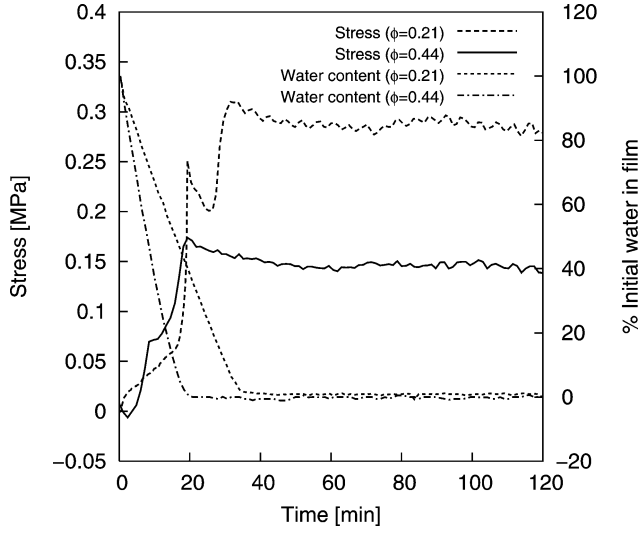


Fig. 5. The drying stress and water content as functions of the drying time for the binary films containing calcium carbonate and deformable latex particles.

It is worth noting that the stress curves in Fig. 5 represent the only case in this study where the sample with low initial solids loading reaches a higher stress than a suspension at a high initial solids loading. The difference in particle size between the calcium carbonate and latex particles makes it possible for the latex particles to migrate toward the air–liquid interface along with the pore liquid during the consolidation phase. Suspensions of low initial solids loading often segregate more, due to the higher mobility of the particulate phase. We believe that this migration yields a denser calcium carbonate–latex network at the surface. This results in a smaller pore size, giving a higher residual stress. The rigid latex particles may migrate toward the surface in a similar fashion, but they will not deform and coalesce and, thus, exert a negligible influence on the residual stress.

### 3.3. Effect of carboxymethylcellulose

The stress evolution and weight loss as a function of time for binary films containing calcium carbonate and soluble CMC binder is shown in Fig. 6. The drying stress evolution displays two separate stress regions, a small initial peak and a large final plateau, which suggest that there are two separate stress-inducing processes. The films containing CMC lost 60% and 12% of the pore liquid at the first peaks for the low and high $\phi_{\text{initial}}$ samples, respectively, and at the point of maximum stress, $\sigma_{\max}$, 96% and 98% had evaporated. The volume fraction of the film at the first stress peak is ∼40% and ∼47% and the stress is ∼0.24 and ∼0.55 MPa for the low and high $\phi_{\text{initial}}$ samples, respectively. At the residual stress plateau, the maximum stress is ∼1.0 and ∼2.3 MPa for the low and high $\phi_{\text{initial}}$ samples, respectively. The evaporation rate is constant throughout the drying process and little stress relaxation is observed beyond the point of maximum stress; the final stress at 120 min is nearly equivalent to the maximum stress value.

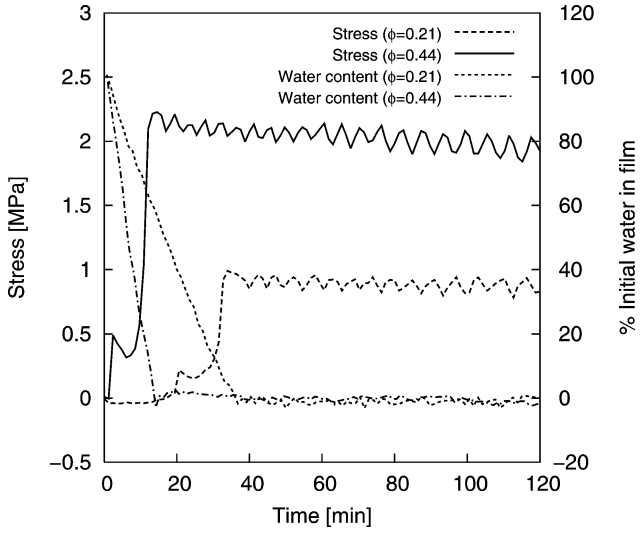


Fig. 6. The drying stress and water content as functions of the drying time for the binary films containing calcium carbonate and CMC.

By comparison of the drying stress curves for pure $CaCO_3$ coatings and the binary $CaCO_3$-CMC coatings in Fig. 7, it is clear that the first stress peaks coincide almost perfectly. Hence, the stress evolution during the first stage of drying is similar for the suspensions with and without addition of CMC, which indicates that the first stress peak is induced by the capillary pressure inside the pores. As the binary coating continues to dry, it reaches the semidry state in which the liquid phase still contains soluble CMC species. It has been shown [22,23] that CMC does not adsorb onto the calcium carbonate particles provided that the dispersion is already stabilized with NaPA. However, the CMC will deposit on the particle surfaces as the remaining liquid evaporates. Previous work on the stress development in tape-cast layers with soluble organic binders [6] showed that the residual stress is related to the shrinkage of the binder beyond the solidification point. Consequently, shrinkage of the CMC-rich regions in the granular film is expected to induce a residual stress in a similar fashion.

Fig. 8 shows the drying stress evolution for a pure CMC film cast from a concentrated CMC solution together with the variation in relative humidity. Drying a pure CMC film can induce very high tensile stresses—up to 35 MPa—but more importantly, a mere humidity oscillation of 3% RH results in a 25-MPa oscillation in stress. The tensile stress for films cast from polymer solutions originates from the volume change caused by evaporation. Croll [24] showed that the residual internal stress is a function of the Young's modulus ($E$) of the film and the volume fraction of solvent in the film at the solidification point ($\phi_s$) and in the dry state ($\phi_r$), according to

$$\sigma = \frac{E}{1-\nu}\frac{\phi_s - \phi_r}{3(1-\phi_r)}, \tag{4}$$

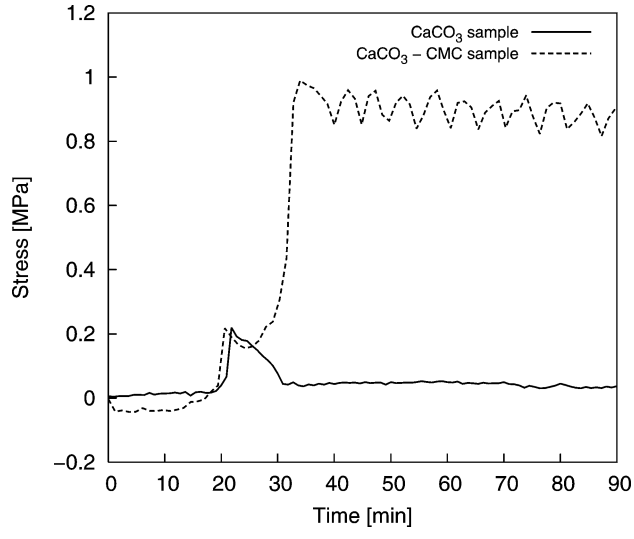


Fig. 7. The drying stress as a function of the drying time for a pure calcium carbonate film and binary films containing CMC at low initial solids loading, $\phi_{\text{initial}} = 0.21$.

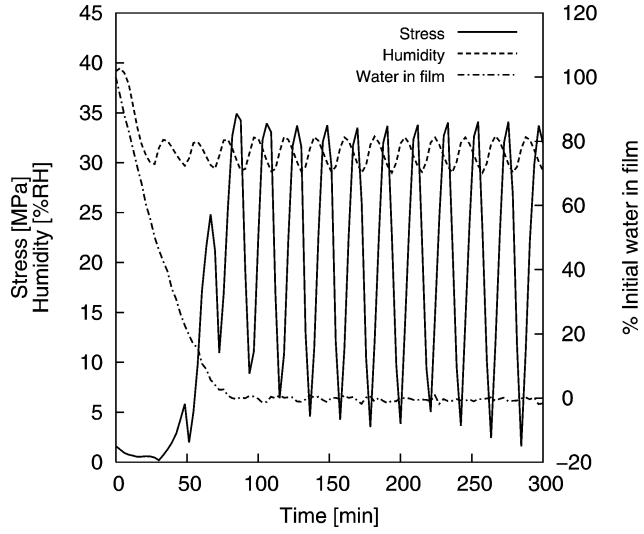


Fig. 8. The drying stress, water content, and relative humidity as functions of the drying time for a pure CMC film cast from an 8 wt% solution of CMC.

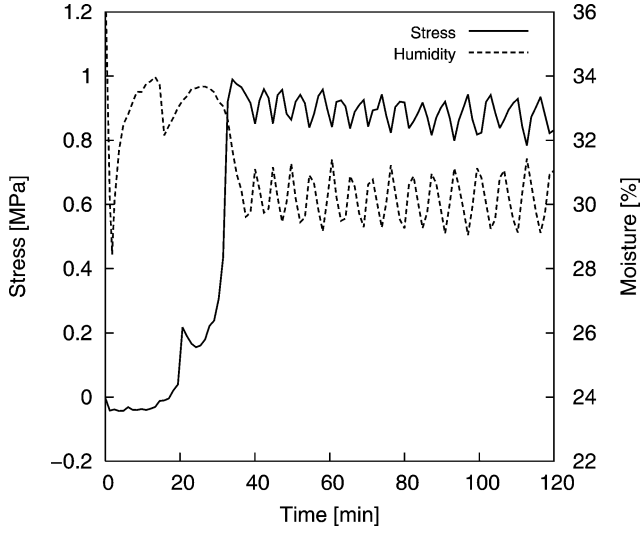


Fig. 9. The drying stress and relative humidity as functions of the drying time for a binary film containing calcium carbonate and CMC with a low initial solids loading ($\phi_{\text{initial}} = 0.21$).

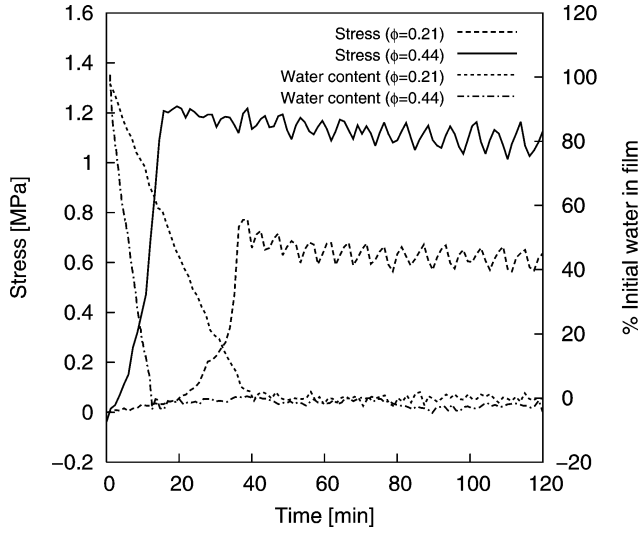


Fig. 10. The drying stress and water content as functions of the drying time for ternary films containing calcium carbonate, deformable latices, and CMC.

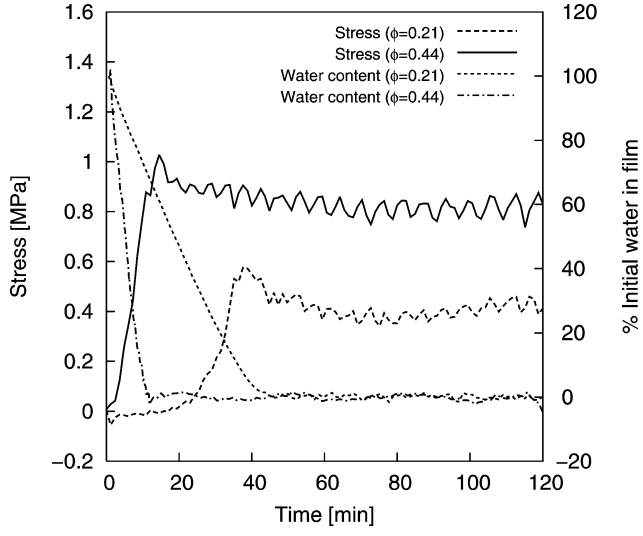


Fig. 11. The drying stress and water content as functions of the drying time for ternary films containing calcium carbonate, rigid latices, and CMC.

where $\nu$ is Poisson's ratio. The absorption and evaporation of water from the film will induce volume changes. The water will also act as a plasticizer for the polymer, thereby reducing its Young's modulus. Hence, Eq. (4) suggests that small volume changes together with changes in Young's modulus can account for drastic changes in stress.

Fig. 9 shows the stress curve for binary coatings containing calcium carbonate and CMC together with the variation in relative humidity. We find that these binary coatings exhibit an oscillatory variation in stress at the residual stress plateau and that the frequency of the stress variation is related to variations in relative humidity in the sample chamber. An increase in humidity results in a decrease in tensile stress and vice versa. We attribute these effects to absorption and evaporation of water; such events will affect the volume and Young's modulus of the CMC phase within the film leading to similar stress changes as observed for the pure CMC films.

The stress evolution and weight loss as a function of time when adding deformable and rigid latex particles to the calcium carbonate–CMC suspensions are shown in Figs. 10 and 11, respectively. We find that the addition of deformable latices (Fig. 10) reduces the maximum stress compared to the films containing only calcium carbonate and CMC (Fig. 6). The maximum stress is ∼0.77 and ∼1.21 MPa and ∼96% and ∼100% of the pore liquid has evaporated at $\sigma_{\max}$ for the low- and high-$\phi_{\text{initial}}$ samples containing deformable latices, respectively. The addition of rigid latices (Fig. 11) further reduces the maximum stress to ∼0.60 and

$\sim$1.03 MPa and the pore liquid has evaporated to $\sim$93% and $\sim$100% at $\sigma_{max}$ for the low- and high-$\phi_{initial}$ samples, respectively. The contribution of the capillary-induced stress to the drying stress evolution is modest for the samples with low initial solids loading and is negligible for the samples with high initial solids loading. The evaporation rate is constant throughout the drying process and some stress relaxation is observed beyond the point of maximum stress; the final stress at 120 min is slightly lower than the maximum stress value.

We find that the residual stress of the ternary coatings varies as a function of the relative humidity in a fashion similar to those observed for the calcium carbonate–CMC coatings in Fig. 9, suggesting that the stress induced by the CMC addition dominates the response. The ternary coatings contain slightly less CMC than the calcium carbonate–CMC systems, resulting in a reduced maximum stress. The absence of the first capillary-induced stress peak may reflect a lower surface tension of the pore liquid in the presence of surfactant-rich latices. These surfactant species may also serve as a plasticizer for the CMC phase, yielding a lower elastic modulus, which would further reduce the stress induced by the CMC. The maximum stress in the films containing deformable latices is greater than that in the corresponding film containing rigid latices. This indicates that the stress induced by the volume changes in the CMC phase during drying is somewhat additive to the stress induced by the coalescence of the deformable latex particles.

## 4. Summary and conclusions

The influence of latex and carboxymethylcellulose binders on the drying stress development of calcium carbonate-based coatings has been studied. We find that pure calcium carbonate coatings display a drying evolution characterized by a sharp capillary-pressure-induced stress peak followed by a rapid stress relaxation and a low residual stress. Binary coatings containing calcium carbonate and rigid latex particles display analogous behavior, because the rigid latices do not coalesce during film formation. In contrast, binary coatings containing calcium carbonate and deformable latices display an initial stress peak induced by capillary pressure and show a stress plateau originating from the coalescence of these deformable species. Addition of the soluble polymer, CMC, result in a two-step stress development process, where the initial capillary-induced stress peak is followed by a second stress rise, a higher stress that do not relax. This large residual stress is attributed to the precipitation of CMC during drying. The shrinkage of the CMC-rich regions in the granular film in the final stages of drying will result in very large tensile stresses. Further, the CMC phase is quite hygroscopic, such that small variations in relative humidity in the drying chamber result in large variations in stress both for pure CMC films and binary ($CaCO_3$–CMC) and ternary ($CaCO_3$–latex–CMC) coatings. The presence of both latex and CMC in the ternary coatings results in a stress history that appears to be somewhat additive reflecting contributions from both latex coalescence and CMC precipitation.

The most important feature of our work is the dramatic increase that minor CMC additions cause on the drying stress evolution, in terms of both maximum stress and residual stress. Since CMC is a common viscosifying aid in both paper and board coatings, such large drying stresses may induce stress-related defects such as curling, cracking, and delamination during manufacturing [25,26]. Based on our observations and related work [12,24], it is likely that such effects would arise from the presence of other soluble organic additives such as ethyl hydroxyethylcellulose (EHEC), starch, and polyvinyl alcohol (PVA).

## Acknowledgments

The authors are grateful to Dr. Nigel Sanders of Specialty Minerals for providing the PCC powder. This work is a part of the Surface Treatment Research Programme at Karlstad University. P.W., J.D., and L.B. acknowledge the financial support of the Swedish Pulp and Paper Research Foundation, the Foundation for Knowledge and Competence Development, and the Swedish Agency for Innovation Systems (VINNOVA). C.J.M. and J.A.L. acknowledge the financial support of the U.S. Department of Energy, Division of Materials Science, under Award DEFG02-91ER45439, through the Frederick Seitz Materials Research Laboratory at the University of Illinois at Urbana–Champaign.

## References

[1] M. Karlsson (Ed.), Papermaking, Part 2, Drying, in: Papermaking Science and Technology, vol. 9, Fapet Oy, Helsinki, 2000.
[2] P. Heikkilä, P. Rajala, E. Lehtinen (Eds.), Pigment Coating and Surface Sizing of Paper, in: Papermaking Science and Technology, vol. 11, Fapet Oy, Helsinki, 2000, pp. 543–565.
[3] D.Y. Perera, J. Coat. Technol. 56 (716) (1984) 111.
[4] C. Petersen, C. Heldmann, D. Johannsmann, Langmuir 15 (1999) 7745.
[5] G.N. Howatt, R.G. Breckenridge, J.M. Brownlow, J. Am. Ceram. Soc. 30 (8) (1947) 237.
[6] J.A. Lewis, K.A. Blackman, A.L. Ogden, J.A. Payne, L.F. Francis, J. Am. Ceram. Soc. 79 (12) (1996) 3225.
[7] R.C. Chiu, T.J. Garino, M.J. Cima, J. Am. Ceram. Soc. 76 (9) (1993) 2257.
[8] R.C. Chiu, M.J. Cima, J. Am. Ceram. Soc. 76 (11) (1993) 2769.
[9] J.J. Guo, J.A. Lewis, J. Am. Ceram. Soc. 82 (9) (1999) 2345.
[10] C.J. Martinez, J.A. Lewis, Langmuir 18 (2002) 4689.
[11] J.A. Payne, A.V. McCormick, L.F. Francis, Rev. Sci. Instrum. 68 (12) (1997) 4564.
[12] Payne J.A. Stress Evolution in Solidifying Coatings, Ph.D. thesis, University of Minnesota, 1998.
[13] E.M. Corcoran, J. Paint Technol. 41 (538) (1969) 635.
[14] J.E. Smay, J.A. Lewis, J. Am. Ceram. Soc. 84 (11) (2001) 2495.
[15] G.W. Scherer, J. Am. Ceram. Soc. 73 (1) (1990) 3.
[16] T.K. Sherwood, Ind. Eng. Chem. 21 (10) (1929) 976.
[17] D.F. Evans, H. Wennerström, The Colloidal Domain, second ed., Wiley–VCH, New York, 1999.

[18] J.M. Coulson, J.F. Richardsson, Particle Technology and Separation Processes, fourth ed., in: Chemical Engineering, vol. 2, Pergamon, Oxford, 1991.
[19] D.R. Lide (Ed.), CRC Handbook of Chemistry and Physics, 73rd ed., CRC Press, Boca Raton, FL, 1992.
[20] D.P. Sheetz, J. Appl. Polym. Sci. 9 (1965) 3759.
[21] A.F. Routh, W.B. Russel, Langmuir 15 (22) (1999) 7762.
[22] K. Backfolk, S. Lagerge, J.B. Rosenholm, D. Eklund, J. Colloid Interface Sci. 248 (2002) 5.
[23] C. Kugge, J. Daicic, I. Furó, The science of papermaking, in: J. Brander (Ed.), Transactions of the 12th Fundamental Research Symposium at Oxford, vol. 2, Pira International, Surrey, UK, 2001, pp. 1183–1202.
[24] S.G. Croll, J. Appl. Polym. Sci. 23 (1979) 847.
[25] E.D. Cohen, E.D. Cohen, E.B. Gutoff (Eds.), Modern Coating and Drying Technology, VCH, New York, 1992, pp. 267–298.
[26] E.B. Gutoff, E.D. Cohen, Coating and Drying Defects: Troubleshooting Operating Problems, in: SPE Monographs Series, Wiley, New York, 1995.